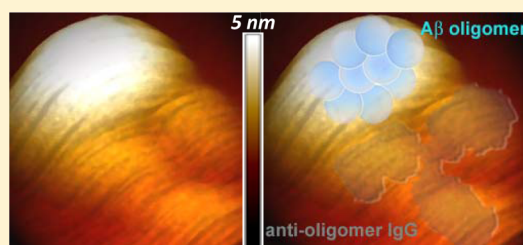


Elucidating Molecular Mass and Shape of a Neurotoxic A $\beta$  OligomerAdriano Sebollela,<sup>\*,†,§,||</sup> Gina-Mirela Mustata,<sup>\*,†,§,⊥</sup> Kevin Luo,<sup>†</sup> Pauline T. Velasco,<sup>†</sup> Kirsten L. Viola,<sup>†</sup> Erika N. Cline,<sup>†</sup> Gajendra S. Shekhawat,<sup>‡</sup> Kyle C. Wilcox,<sup>†</sup> Vinayak P. Dravid,<sup>‡</sup> and William L. Klein<sup>†</sup><sup>†</sup>Department of Neurobiology, Northwestern University, Evanston, Illinois 60208, United States<sup>‡</sup>International Institute for Nanotechnology and NUANCE Center, Department of Materials Science and Engineering, Northwestern University, Evanston, Illinois 60004, United States

## Supporting Information

**ABSTRACT:** Alzheimer's disease (AD), the most prevalent type of dementia, has been associated with the accumulation of amyloid  $\beta$  oligomers (A $\beta$ O) in the central nervous system. A $\beta$ O vary widely in size, ranging from dimers to larger than 100 kDa. Evidence indicates that not all oligomers are toxic, and there is yet no consensus on the size of the actual toxic oligomer. Here we used NU4, a conformation-dependent anti-A $\beta$ O monoclonal antibody, to investigate size and shape of a toxic A $\beta$ O assembly. By using size-exclusion chromatography and immuno-based detection, we isolated an A $\beta$ O-NU4 complex amenable for biochemical and morphological studies. The apparent molecular mass of the NU4-targeted oligomer was 80 kDa. Atomic force microscopy imaging of the A $\beta$ O-NU4 complex showed a size distribution centered at 5.37 nm, an increment of 1.5 nm compared to the size of A $\beta$ O (3.85 nm). This increment was compatible with the size of NU4 (1.3 nm), suggesting a 1:1 oligomer to NU4 ratio. NU4-reactive oligomers extracted from AD human brain concentrated in a molecular mass range similar to that found for in vitro prepared oligomers, supporting the relevance of the species herein studied. These results represent an important step toward understanding the connection between A $\beta$ O size and toxicity.

**KEYWORDS:** A $\beta$  oligomer, Alzheimer's disease, NU4 antibody, neurotoxicity, AFM



Alzheimer's disease (AD), the most prevalent type of dementia throughout the world, is characterized by striking memory loss followed by widespread cognitive failure and death.<sup>1</sup> The major histopathological hallmark of AD is the accumulation of amyloid plaques in the brain, composed of amyloid  $\beta$  peptides (A $\beta$ ) of 40–42 amino acids, which are generated through sequential cleavage of the transmembrane glycoprotein APP (reviewed in ref 2). In addition to A $\beta$  plaques, which are primarily composed of A $\beta$  in fibrillar, insoluble state, soluble A $\beta$  oligomers have also been associated with AD pathology.<sup>3,4</sup> In fact, strong evidence accumulated in recent years implicates A $\beta$  oligomers (A $\beta$ O), also known as A $\beta$ -derived diffusible ligands (ADDLs), rather than insoluble fibrils, as the prominent neurotoxins in AD.<sup>5–7</sup>

Despite the vast information accumulated on the effects of A $\beta$  oligomers, no clear demonstration of the size or structure of the actual toxic oligomeric A $\beta$  species has been reported so far. Nonetheless, strong evidence indicates that both oligomer size and conformation play an important role in toxicity.<sup>8–11</sup> While some investigators observed toxicity of low molecular mass oligomers, such as dimers and trimers,<sup>12–16</sup> a strong correlation between higher molecular mass assemblies, such as dodecamers, and AD-linked synaptotoxicity has been reported by others.<sup>17–20</sup> In addition to these assemblies, a number of different A $\beta$  species, including pentamers,<sup>21</sup> 60,<sup>22</sup> 80,<sup>23</sup> and 150 kDa species<sup>24</sup> have also been detected in vitro or extracted from AD brains. These difficulties in identifying the actual toxic A $\beta$

oligomeric assembly have direct implications in elucidating AD mechanisms and drug development.

An attractive and currently available tool to isolate specific A $\beta$  species in solution is the use of conformation-sensitive monoclonal antibodies targeting A $\beta$ O. These antibodies have been isolated by different groups<sup>25,26</sup> and recognize specific conformational epitopes on oligomeric A $\beta$ . One of the most studied anti-A $\beta$ O monoclonals, NU4, was shown to discriminate AD from control human brain extracts and to protect neurons in culture from A $\beta$ O-induced ROS generation,<sup>26</sup> clearly indicating the capacity of NU4 to bind A $\beta$  species relevant to AD pathology.

Here we have used NU4 to isolate and study biochemical and morphological aspects of a particular, toxic A $\beta$ O species. Using a combination of size-exclusion chromatography (SEC) and atomic force microscopy (AFM), we were able to determine the molecular mass and z-height of the A $\beta$ O preferentially targeted by NU4. Acquiring data on the conformation of toxic A $\beta$ O may accelerate the development of more specific and efficient therapeutic and diagnostic approaches to AD-associated A $\beta$  neurotoxicity.

Received: July 18, 2014

Revised: October 23, 2014

Published: October 24, 2014

## RESULTS AND DISCUSSION

Although it has been established that  $A\beta$ O play a central role in AD pathogenesis, the molecular identity of the oligomeric form of  $A\beta$  most germane to disease has yet to be determined. Previous work indicated that a high molecular mass assembly (roughly a 12-mer), rather than low-order  $A\beta$ O, is primarily responsible for the neuronal attack suffered by neurons exposed to  $A\beta$ O.<sup>18,19</sup> By using complementary biochemical and imaging techniques, we have been able to elucidate the size and shape of this high molecular mass, neurotoxic oligomer specimen.

### Monoclonal Antibody NU4 Interacts with $A\beta$ Oligomer Species Bearing Neuronal Binding Activity.

NU4 is a monoclonal anti- $A\beta$ O antibody known to be conformation sensitive; that is, it preferentially interacts with self-associated  $A\beta$  rather than its monomeric form.<sup>26</sup> Protection against  $A\beta$ O-associated toxicity by NU4 has been reported.<sup>27</sup> For instance, it has been shown that NU4 treatment prior to  $A\beta$ O challenge prevented ROS accumulation in cultured neurons<sup>26</sup> and behavioral deficits in AD transgenic mice,<sup>28</sup> thus implying neurotoxic activity to NU4-reactive oligomers. Here we made use of fluorescently tagged  $A\beta$ O (FAM- $A\beta$ O) to compare the entire population of  $A\beta$  species bound to neurons with that of NU4-targeted oligomers. A robust colocalization between FAM and NU4-based signals on neuronal processes of hippocampal neurons was detected (Figure 1). Along with previous results on the presence of

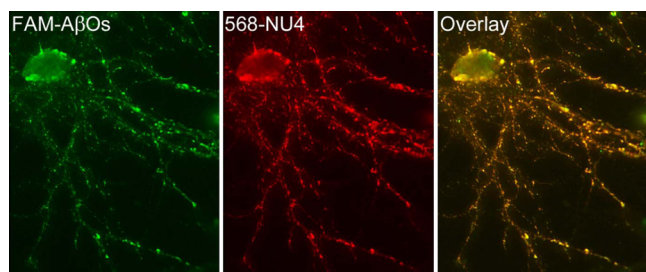


**Figure 1.** Monoclonal anti- $A\beta$ O antibody NU4 targets pathologically relevant  $A\beta$  species. Rat hippocampal neurons in culture were exposed to 500 nM fluorescently labeled  $A\beta$ O (FAM- $A\beta$ O) (green channel) followed by immunolabeling with 568-NU4 (red). The overlay panel shows robust colocalization (yellow) between direct and antibody-based  $A\beta$ O visualization.

$A\beta$ O in culture medium even after 24 h incubation at 37 °C,<sup>29,30</sup> our present result indicates that soluble, neurotoxic  $A\beta$  species reacting with NU4 in the original preparation are abundant and conformationally similar to neuroactive oligomers in culture medium.

**Isolation and Molecular Mass Determination of NU4- $A\beta$  Oligomer Complex.** Typical  $A\beta$ O preparations are known to comprise two major populations eluting at 60–150 kDa (high molecular mass oligomers) and 10–15 kDa (low molecular mass oligomers) on SEC analysis,<sup>18,20,31,32</sup> and to contain only trace amounts of monomers.<sup>33</sup> To determine which population is preferentially targeted by NU4, we performed SEC fractionation combined to immuno-based detection of NU4-targeted oligomers. Comparison between spectrophotometric detection of  $A\beta$ O (Figure 2, red) and dot immunoblot signal from SEC fractions (Figure 2, gray) reveals that NU4 preferentially targets high molecular mass oligomers, since significantly higher dot blot intensities per unit of

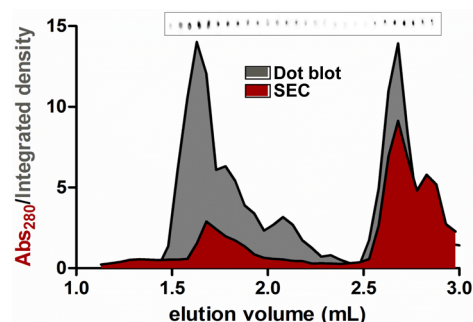


**Figure 2.** NU4 preferentially interacts with high molecular mass oligomers.  $A\beta$ O were fractionated by size exclusion chromatography (monitored by absorbance at 280 nm, red curve), and individual fractions (100  $\mu$ L) were probed for NU4 immunoreactivity by dot blot. A representative dot blot image is shown (top) and its quantification (integrated density) is plotted (gray). Note that high molecular mass oligomers showed significantly higher NU4 immunoreactivity than low molecular mass oligomers when compared to their relative absorbance readings at 280 nm.

absorbance for high molecular mass species were observed, as opposed to similar areas for low molecular mass oligomers.

Taking advantage of the preferential binding of NU4 to higher order oligomers, we sought to determine the apparent molecular mass of NU4-targeted  $A\beta$ O by SEC based on the elution volume shift (thus the mass shift) of the antibody upon  $A\beta$ O binding. The apparent molecular masses of free NU4 and NU4- $A\beta$ O complex obtained by SEC (Figure 3A) were 103 and 182 kDa, respectively. By subtracting these values, we found the apparent molecular mass of the NU4-targeted  $A\beta$ O to be 79 kDa, thus compatible with an 18-mer (assuming a theoretical  $A\beta$  monomer mass of 4.5 kDa and a 1:1 oligomer to NU4 ratio). To verify the presence of both  $A\beta$ O and NU4 in the peak assigned as “ $A\beta$ O+NU4” complex (Figure 3A), we have collected serial fractions surrounding the peak and tested their reactivity against antibodies which specifically detect either  $A\beta$  oligomers ( $\alpha$ - $A\beta$ O polyclonal M69<sup>34</sup>) or NU4 ( $\alpha$ -IgG; commercially available anti-mouse IgG) by dot blot. A similar pattern of increasing reactivity toward the center of the peak was observed on both membranes (Figure 3A), indicating that  $A\beta$ O and NU4 indeed coelute in that peak. Unbound NU4 appears as a minor peak in the “ $A\beta$ O+NU4” curve eluting at a similar volume as control NU4 (black). Although a slight shift (0.03 mL) in elution volume of these peaks assigned as NU4 was observed, which in theory could be attributed to an interaction between NU4 and low molecular mass  $A\beta$ O, the lack of shift in the peak corresponding to low molecular mass  $A\beta$ O (which is attributed to species ranging from dimers to tetramers; see ref 26) upon interaction with NU4 (Figure 3A, inset) indicates that NU4 indeed preferentially interacts with high molecular mass  $A\beta$ O.

Molecular mass of NU4-targeted  $A\beta$ O was directly evaluated using fluorescently labeled NU4 (568-NU4). A shift in elution volume of peak corresponding to NU4 upon interaction with  $A\beta$ O was observed (Figure 3B), and was compatible with that obtained using unlabeled NU4 (Figure 3A). In addition,  $A\beta$ O (in the absence of NU4) subjected to centrifugal filtration were able to pass through a 100 kDa MWCO membrane, as indicated by the absence of signal in the retentate recovered after filtration (Figure 3C). This result gives evidence that high molecular mass oligomers are indeed smaller than 100 kDa, as previously indicated by subtracting the apparent molecular

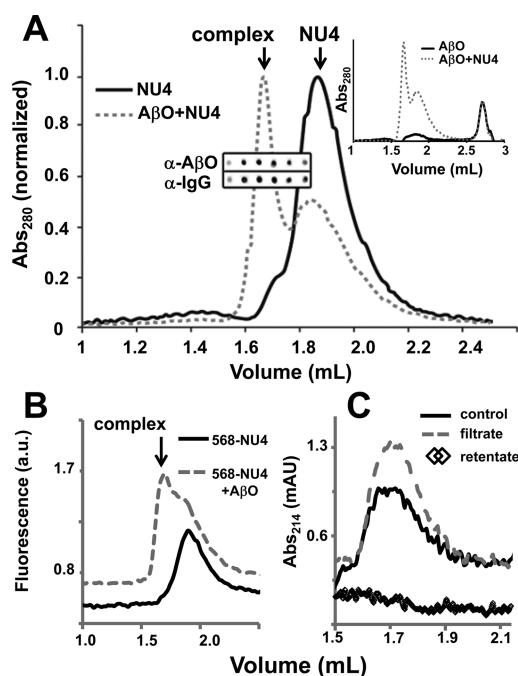


**Figure 3.** Apparent molecular mass of large  $A\beta$ O s targeted by NU4 is 80 kDa. NU4 or  $A\beta$ O-NU4 mixtures (molar ratio 1:100 NU4: $A\beta$ ) were separated by size exclusion chromatography (A). The apparent molecular mass of the  $A\beta$ O-NU4 complex was assessed based on the shift in elution volume before (solid) or after (dotted) incubation with  $A\beta$ O s. Presence of  $A\beta$ O s and IgG in each fraction was assessed by dot immunoblot probed with NU4 or anti-mouse IgG, respectively. Difference in elution volume of major peaks was used to calculate oligomer mass. A representative run including the region where low molecular mass oligomers elute is shown in the inset. (B) Apparent molecular mass of  $A\beta$ O-NU4 complex was alternatively determined using fluorescently tagged NU4 (568-NU4). In this case, SEC was performed using an Agilent 1100 HPLC instrument equipped with a fluorescence detector. Note the presence of complex eluting at the same elution volume as in (A). (C) High molecular mass  $A\beta$  oligomers are smaller than 100 kDa.  $A\beta$ O s and the filtrate and retentate from 100 kDa MWCO centrifugal filtration were subjected to SEC to detect the presence of high molecular mass  $A\beta$  oligomers. Only the region corresponding to elution volume for high molecular mass oligomers is shown.

masses of NU4/ $A\beta$ O complex and free NU4. The higher signal in the filtrate compared to control  $A\beta$ O sample (not subjected to filtration) is likely due to an error associated with volume correction after concentration of the sample on the membrane during centrifugal filtration.

Further evidence on the interaction between  $A\beta$ O and NU4 was obtained using native PAGE as a complementary method to SEC. For this sake,  $A\beta$ O-NU4 complex molecular mass was analyzed by native PAGE (Supporting Information Figure 1).  $A\beta$ O s migrate as previously observed on native PAGE,<sup>31</sup> while NU4 runs as a single band at a MW significantly higher than expected. This abnormal migration of NU4 is likely due to the neutral to basic pI of IgGs (between 7 and 9),<sup>35</sup> which makes these molecules only slightly charged in the pH of running buffer (8.3). When  $A\beta$ O s and NU4 are mixed, an interaction can be readily detected by the presence of a slow migrating, diffuse band (left panel, red box). The presence of NU4 in this diffuse band was confirmed by Western blot with anti-mouse IgG (right, red box). The faster migration of the band front corresponding to complex compared to NU4 alone is likely due

to the influence of charged groups from  $A\beta$  to the net charge of the complex. Thus, although the native PAGE data corroborates the formation of a soluble complex between  $A\beta$  oligomer and NU4, it is limited in providing information on the molecular mass of  $A\beta$ O-NU4 complex and, consequently, of NU4-targeted  $A\beta$  oligomer.

The specificity and stability of the NU4- $A\beta$ O complex was further analyzed. No elution volume shift was observed when  $A\beta$ O s were incubated with a nonimmune control IgG (Figure 4A). Interestingly, preincubation of  $A\beta$ O s with 1% Triton X-

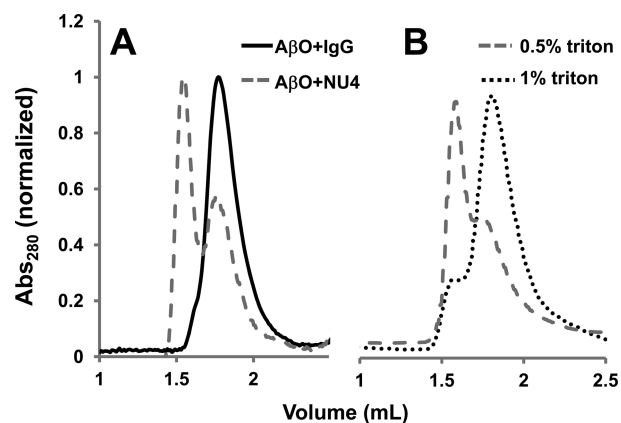


**Figure 4.** Conformational dependence of the interaction between NU4 and  $A\beta$  oligomer. (A)  $A\beta$ O s (10  $\mu$ M) were incubated with either NU4 (gray, dashed) or nonimmune control IgG (black) for 30 min at 4  $^{\circ}$ C before SEC. Note that no molecular mass shift was observed when  $A\beta$ O s were incubated with control IgG. (B)  $A\beta$ O s were preincubated with either 0.5% (gray, dashed) or 1% (black, dotted) Triton X-100 for 5 min at RT before addition of NU4 and SEC as in (A). A significant prevention of complex formation is observed when 1% Triton X-100 was added.

100, a condition known to not affect antigen-antibody reactions, was able to disrupt  $A\beta$ O-NU4 complex stability (Figure 4B), suggesting the existence of a detergent-sensitive structure on this  $A\beta$ O species that is important for  $A\beta$ O-targeting by NU4.

Taken together, these data indicate that the conformation-sensitive monoclonal anti- $A\beta$  oligomer NU4 targets a single  $A\beta$  oligomeric species, a feature that may be used to overcome the limitation in studying toxic oligomer structure in complex samples. It is important to emphasize, however, that our current approach is limited in terms of accuracy of molecular mass determination, due to the imprecision inherent to the SEC technique.

**Morphology of NU4- $A\beta$  Oligomer Complex by AFM.** SEC fractions from high molecular mass  $A\beta$ O s, NU4, and NU4- $A\beta$ O complex peaks were collected and observed by AFM (Figure 5). Under low magnification, both fractionated  $A\beta$ O s (Figure 5A) and NU4- $A\beta$ O complex (Figure 5B) samples presented structures highly homogeneous in height (0.6 and 1.1 nm standard deviation of z-height for  $A\beta$ O s and complex samples, respectively; 24–35 specimen analyzed per condition). On the other hand, while the fractionated  $A\beta$ O s showed to be similar in shape, in the NU4- $A\beta$ O complex sample, the specimens observed presented various shapes, likely due to variations on the position the complex adsorbed to mica.

High resolution images of NU4 revealed a trilobar structure (Figure 5C) similar to previously published structures of IgG molecules.<sup>36,37</sup> Cross-sectional profiles of this particular

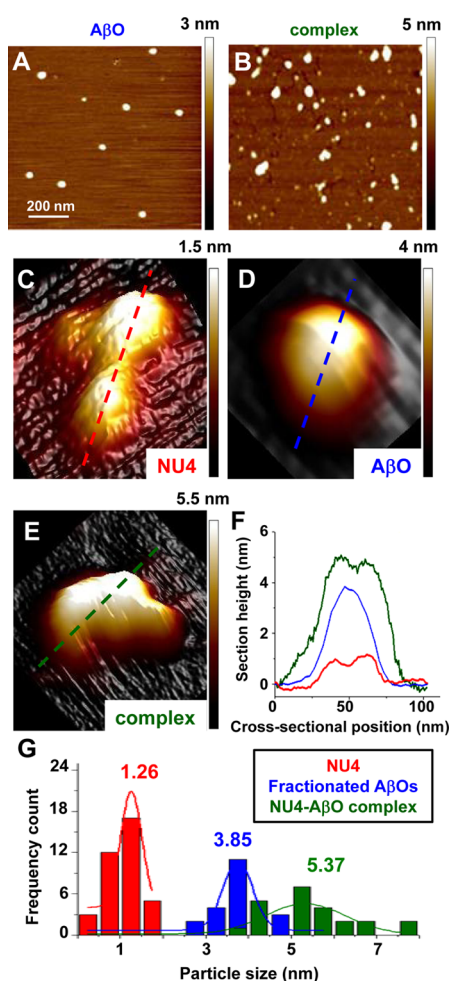


**Figure 5.** A $\beta$  oligomer-NU4 complex visualized by AFM. NU4 antibody, high molecular mass A $\beta$  oligomers (A $\beta$ Os), or NU4-A $\beta$ O complex were fractionated by SEC and immediately adsorbed to mica surface for analysis. Low resolution ( $1 \times 1$  microm<sup>2</sup> scans) of SEC-fractionated high molecular mass A $\beta$ Os (A) and NU4-A $\beta$  oligomer complex (B) and high resolution representative images of NU4 (C), high molecular mass A $\beta$ Os (D), or NU4-A $\beta$ O complex (E) are presented. z-Height profiles for each sample are shown in (F). SEC elution volumes for fractions were as follows: NU4, 1.8 mL; A $\beta$ O-NU4 complex, 1.6 mL, based on a run similar to that shown in Figure 3A; and high molecular mass A $\beta$ Os, 1.7 mL, based on a run similar to that shown in Figure 2. (G) Size distribution analysis of the selected specimens in each sample. When NU4 was present, only the trilobar structures were considered (denatured or single lobe structures were excluded).

structure rendered a z-height of 1.15 nm (Figure 5F), also consistent with the reported size for IgG. When observed at high magnification, high molecular mass A $\beta$ Os showed globular structures of homogeneous size and shape (Figure 5D). The diameter, measured as height in the cross-sectional profile, was 3.93 nm (Figure 5F). Although we have opted to not report the measured width of the observed specimen, due to errors introduced by the inconsistent width of the imaging tip, based on the homogeneity in z-height of fractionated large A $\beta$ O (Figure 5A), we concluded that these oligomeric species present a globular shape, since elongated molecules should render two distinct height populations depending on the way it lands on mica surface. Detecting a singular height population implies a spherical symmetry of the specimen. Alternatively, by

using the Porath plot<sup>38</sup> and our current SEC data, we have found the hydrodynamic radius (Stokes radius) of high molecular mass A $\beta$ Os to be 4.8 nm, assuming a globular-shape-like behavior of this assembly in solution. Although this value is around 1 nm higher than the z-height calculated from our AFM data, we consider the two measurements as being in good agreement, since this difference may reflect changes in structure induced by the sample preparation for AFM, as the drying process is known to decrease the measured size.<sup>39,40</sup> Moreover, our results are in line with previous AFM studies using nonfractionated A $\beta$ Os, in which globular oligomers of  $5 \pm 3$  nm were visualized.<sup>31,41,42</sup> The narrower size distribution of oligomers in our analysis ( $3.85 \pm 0.67$  nm, Figure 5G) is due to the SEC fractionation which limited the specimen analyzed to a subpopulation of high molecular mass oligomers, compared to unfractionated A $\beta$ O samples used in previous studies.

Although images of the NU4-A $\beta$ O complex showed structures with irregular shapes and a wider range of sizes (Figure 5B), including spherical features of lower height profile, which can be attributed to unbound (NU4 free) oligomers, the cross-sectional profile of a representative complex (Figure 5E) showed a strong similarity with the shape of the antibody. In fact, in this structure, a fourth lobe is present, strengthening the notion that a complex between NU4 and a single, high mass A $\beta$  oligomer species is formed in solution. A statistical analysis of the size of the observed structures is presented in Figure 5G. After analyzing 24–35 structures per condition, the average height of the antibody was found to be 1.26 nm ( $\pm 0.37$  nm). The average diameter of high molecular mass oligomers was found to be 3.85 nm ( $\pm 0.67$  nm), while the NU4-A $\beta$ O complex averaged a height of 5.37 nm ( $\pm 1.1$  nm). Interestingly, this increment in height (approximately 1.5 nm) is consistent with a 1:1 stoichiometry in the interaction between NU4 and A $\beta$ O. In conjunction with the relatively narrow size distribution for the NU4-A $\beta$ O complex, this result indicates that NU4 preferentially interacts with a single A $\beta$ O species. As for A $\beta$ Os, we have also calculated the Stokes radius for the A $\beta$ O-NU4 complex using the Porath plot. Again, radius (7.9 nm) was slightly larger than the z-height for the same complex as measured by AFM, what may be attributed to dehydration during sample preparation for AFM. It is important to note, however, that the difference in radii between free and NU4-complexed high mass A $\beta$ O, around 3 nm, is consistent with the 1:1 stoichiometry pointed out above, considering the well-known Stoke radius of IgG molecules (around 5 nm).

**Molecular Mass of NU4-Reactive Oligomers in AD Human Brain Extracts.** To gain insight into the relevance of NU4-targeted high mass A $\beta$  oligomer to AD pathology, we have evaluated the presence of NU4-reactive oligomers of similar molecular mass in nondenatured AD human brain extracts. Dot blot analysis carried out after centrifugal filtration of extracts from either cortex or cerebellum revealed that NU4-targeted species concentrates between 50 and 300 kDa in the cortex, while no significant signal was detected in extracts from cerebellum (Figure 6), a region known to not accumulate A $\beta$ Os.<sup>17</sup> This indicates that NU4 reactivity in the cortex indeed comes from A $\beta$ Os, and that it mainly comes from a species sized in a molecular mass range compatible with our data using in vitro prepared A $\beta$ Os. Moreover, the molecular mass range found for this large A $\beta$ O is in agreement with previous data obtained from human AD brain extracts in which a major 80 kDa species has been reported.<sup>23</sup>

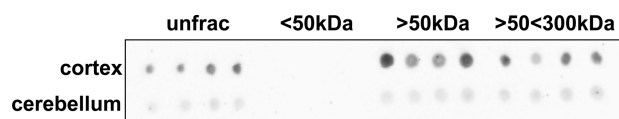


**Figure 6.** Size of NU4-targeted  $A\beta$  oligomers in Alzheimer diseased human brain. Extracts from either frontal cortex or cerebellum were prepared from post-mortem tissue from an AD definite case and tested for its immunoreactivity to NU4 antibody by dot blot. After centrifugal filtration under the indicated MWCO filter, 1  $\mu$ g (total protein) was spotted onto a nitrocellulose membrane in quadruplicate. Peroxidase treatment (3%  $H_2O_2$ , 20 min) was carried out to eliminate endogenous peroxidase signal. Membrane was then probed with NU4 (1  $\mu$ g/mL) for 2 h at RT, followed by incubation with HRP-conjugated secondary antibody; and signal revealed by chemiluminescence. Unfrac corresponds to input supernatant.

In this work, we report a detailed characterization of a complex between NU4, a conformational monoclonal antibody known to prevent  $A\beta$ O toxicity in vitro and in vivo, and  $A\beta$  oligomers. The strategy relied on the specificity of NU4 targeting for the isolation and visualization of the antibody-oligomer complex by SEC and AFM, respectively. When applied to a classic  $A\beta$  oligomer preparation known to comprise multiple species, this approach allowed us to determine the apparent molecular mass of a high- $n$  oligomer retaining neuronal binding activity. Furthermore, we were able to directly observe the antibody-oligomer complex using high resolution AFM. We showed that the size distribution of the  $A\beta$ O-NU4 complex is narrower than expected, considering the multitude of  $A\beta$  species reported, supporting a preferential binding of NU4 to a specific, 4 nm globular oligomeric assembly. Our AFM data is further supported by the typical trilobar structure of IgG molecules found in NU4-containing samples. Interestingly, the AFM images of the  $A\beta$ O-NU4 complex showed a 1:1 stoichiometry and the individual shapes of  $A\beta$ O and NU4 seem to be preserved in the complex. However, given the complexity of the mechanism underlying  $A\beta$  self-assembly, we must emphasize that studies using more accurate techniques such as SAXS or X-ray crystallography may reveal different aspects of this interaction. These refined analyses should be pursued in future works. Moreover, also considering the complex relationship between  $A\beta$  self-assembly and toxicity, we highlight that the main contribution of this work is the description of a novel approach to isolate and characterize a specific oligomeric species, in this particular case, an  $A\beta$  assembly proven to be neurotoxic, instead of claiming the existence of a single neurotoxic oligomer species responsible for the entire spectrum of AD pathology. The relative contribution of this NU4-targeted  $A\beta$ O to AD pathology, as well as the toxic cascade triggered by this high mass  $A\beta$  assembly, remains to be fully elucidated. For instance, it is important to evaluate the toxicity of isolated NU4-targeted  $A\beta$ O. Unfortunately, to date, no assay to recover oligomers from an antibody complex without affecting oligomer structure has been developed. We propose, however, that the approach employed here may be useful for the isolation of particular oligomeric species directly from Alzheimer's disease brain extracts, as well as oligomers responsible for other degenerative disorders, such as Parkinson's disease and prionoses, for biochemical and biophysical studies.

## METHODS

**Chemicals.** Purified monoclonal antibodies (NU1 and NU4) were obtained as previously described.<sup>26</sup>  $A\beta_{1-42}$  was from American Peptide. Other reagents were from Sigma Chemical or Merck unless otherwise indicated.

**$A\beta$  Oligomers.** Oligomers were prepared according to Chromy et al.<sup>31</sup>  $A\beta_{1-42}$  peptide was monomerized in hexafluoroisopropanol, aliquoted, evaporated, and stored as a solid film at  $-80^\circ\text{C}$ . The peptide film was resuspended in anhydrous dimethyl sulfoxide to 5 mM. The 5 mM peptide stock was diluted to a concentration of  $\sim 100$   $\mu\text{M}$  with the addition of F12 medium without phenol red (Caisson Laboratories). The solution was vortexed thoroughly and incubated for 24 h at  $4^\circ\text{C}$ . Following incubation, the solution was centrifuged at  $14\,000g$  for 10 min at  $4^\circ\text{C}$ . Supernatant, which comprises  $A\beta$ O, was transferred to a new tube and stored at  $4^\circ\text{C}$ . Fluorescently labeled  $A\beta$ O were prepared using a 4:1 mixture of unlabeled  $A\beta$  and FAM- $A\beta_{1-42}$  peptide (AnaSpec) as described in Pitt et al.<sup>43</sup> Oligomers were used within 24 h after preparation.

**Fluorescent Conjugation of NU4 Antibody.** NU4 antibody was fluorescently tagged using the Alexa Fluor 568 Protein Labeling Kit (Invitrogen) and following manufacturer's instructions.

**Primary Rat Hippocampal Neuron Cultures.** All animals were handled in accordance with national guidelines laid down by the NIH regarding care and use of animals for experimental procedures. In brief, a timed pregnant Sprague-Dawley rat, gestation day 18, was anesthetized by  $\text{CO}_2$  inhalation, using a slow flow rate to minimize anxiety. Immediately after anesthetization, the mother was decapitated, and the uterine sac removed and placed on ice. The embryos, anesthetized by cold, were removed from the sac, decapitated, and their hippocampi removed and placed into ice-cold Hibernate medium. Hippocampal neurons were cultured according to Brewer et al.<sup>44</sup> and maintained in Neurobasal medium supplemented with B27 (Invitrogen) for at least 18 days before treatments.

**Immunocytochemistry.** Cells were incubated with vehicle or FAM- $A\beta$ O (500 nM) for 60 min at  $37^\circ\text{C}$  and fixed with formaldehyde. For immunostaining, cells were blocked in 10% normal goat serum in PBS for 45 min at room temperature, then immunolabeled with 568-NU4 (1  $\mu\text{g}/\text{mL}$  in blocking buffer) overnight at  $4^\circ\text{C}$ . Cells were visualized using a Nikon TE-2000 inverted epifluorescence microscope.

**Size Exclusion Chromatography.** Size-exclusion chromatography (SEC) was conducted similarly to Chromy et al.,<sup>31</sup> using a GPC100 column (Eprogen;  $250 \times 4.6$  mm; recommended MW range 5–160 kDa) connected to an Akta Explorer HPLC apparatus (GE). Cold PBS pH 7.4 (KD Medical, Columbia, MD) was used as the liquid phase at a flow rate of 0.4 mL/min. All the runs were performed in a cold room set to  $+4$ – $8^\circ\text{C}$  and lasted less than 10 min from injection to complete elution. The column was calibrated with the following protein standards (Sigma):  $\beta$ -amylase (220, 1.74); alcohol dehydrogenase (150, 1.84); BSA (66, 1.88); OVA (45, 2.01); carbonic anhydrase (29, 2.30); and RNase (13.7, 2.65). MW and elution volume ( $V_e$ ) for each standard are presented in parentheses. Plasmidial DNA (1.53 mL) was used to calibrate the void volume ( $V_0$ ). Plotted were  $V_e/V_0$  ( $x$ -axis) and log MW. Linear fit rendered  $R^2 = 0.88$ . Elution was monitored by absorbance at both 280 and 214 nm. NU4 (100  $\mu\text{L}$  at 0.1  $\mu\text{M}$ ) or a mixture of  $A\beta$ O and NU4 (100:1 mol ratio, preincubated for 30 min at  $4^\circ\text{C}$ ) was injected, and fractions (typically 100  $\mu\text{L}$ ) were collected in low-protein-binding 96-well plates (Greiner).

**Dot Blot Assay.** Aliquots (1  $\mu\text{L}$ ) from each SEC fraction were spotted on nitrocellulose and the membrane allowed to dry for 15 min before blocking in 5% nonfat dry milk in TBS-T (20 mM Tris-HCl, pH 7.4, 0.8% NaCl, 0.1% Tween-20) for 1 h at RT. The membrane was then incubated with anti- $A\beta$ O antibodies [NU1 or rabbit polyclonal M69/2<sup>34</sup> at 1  $\mu\text{g}/\text{mL}$  for 2 h at RT in blocking buffer]. After washing with TBS-T, bound proteins were visualized using anti-mouse or anti-rabbit IgG HRP-conjugated antibodies (GE; 1:40 000 in blocking buffer) and the SuperSignal West Femto chemiluminescence

kit (Pierce). Quantification was performed using Kodak 1D Image Analysis software for the IS440CF Image Station.

#### Atomic Force Microscopy Sample Preparation and Imaging.

AFM images were acquired using a Multimode atomic force microscope with a Nanoscope V controller (Bruker, Santa Barbara, CA). Imaging was performed in tapping mode in air using silicon probes from Applied Nano with the nominal spring constant of 5 N/m. Image analysis was performed using the NanoScope Analysis software. A droplet of 25–35  $\mu\text{L}$  of the explored solutions ( $A\beta\text{Os}$ , NU4, and  $A\beta\text{Os}$  bound to NU4) was allowed to absorb on freshly cleaved mica for 2–3 min. The excess solution was rinsed twice with ultrapure water in order to remove salt deposits and other residues. The samples were gently dried under  $\text{N}_2$  flow.

**Brain Extracts.** Post-mortem human brain tissue was obtained from the Northwestern Alzheimer's Disease Center (<http://www.Brain.northwestern.edu/research/brain/autopsy.html>). Donor was a male diagnosed with definite AD (CERAD score C, Braak stage VI). Extracts were prepared from either frontal cortex or cerebellum based on the protocol described in Gong et al.<sup>17</sup> For each brain region, a fragment of 200 mg was homogenized in 2 volumes of TBS supplemented with protease inhibitors (Complete mini EDTA-free, Roche) and centrifuged at 10 000g for 10 min. Supernatant was then centrifuged at 100 000g for 1 h at 4 °C. After determination of protein concentration using 660 nm reagent (Pierce, Rockford, IL), the second supernatant was applied to a 50 kDa ultrafiltration unit (Millipore). Retentate was diluted and reapplied to completely remove species smaller than 50 kDa. Final retentate containing proteins larger than 50 kDa was loaded on a 300 kDa ultrafiltration unit (Millipore) and spun to remove species above 300 kDa. For dot blotting, 1  $\mu\text{L}$  was spotted onto dry nitrocellulose membrane and the membrane was treated for 30 min in 0.3%  $\text{H}_2\text{O}_2$  to inactivate endogenous peroxidases in brain homogenate fractions. Following blocking with 5% nonfat dry milk in TBS-T, the membrane was probed with 2.5  $\mu\text{g}/\text{mL}$  NU4 for 2 h at room temperature followed by HRP-conjugated anti-mouse IgG (1:20 000).

## ■ ASSOCIATED CONTENT

### ● Supporting Information

$A\beta\text{O}$ -NU4 complex analyzed by native PAGE. This material is available free of charge via the Internet at <http://pubs.acs.org/>.

## ■ AUTHOR INFORMATION

### Corresponding Authors

\*E-mail: [sebollela@fmrp.usp.br](mailto:sebollela@fmrp.usp.br).

\*E-mail: [mirelaginamustata@gmail.com](mailto:mirelaginamustata@gmail.com).

### Present Addresses

<sup>||</sup>A.S.: Department of Biochemistry and Immunology, Faculty of Medicine at Ribeirão Preto, University of São Paulo, 14049-900 Ribeirão Preto, SP, Brazil.

<sup>⊥</sup>G.-M.M.: Department of Chemistry and Physics, Simmons College, Boston, MA 02115.

### Author Contributions

<sup>§</sup>A.S. and G.-M.M. contributed equally to this work. V.P.D. and W.L.K. laboratories contributed equally to this work. A.S. conceived, designed, and carried out the experiments, analyzed data, and wrote the manuscript. G.-M.M. conceived, designed, and carried out the experiments, analyzed data, and wrote the manuscript. K.L. carried out experiments, analyzed data, and helped edit the manuscript. P.T.V. contributed to experimental plans, consulted on data interpretation, purified NU4 antibody, and helped edit the manuscript. K.L.V. performed experiments, analyzed data, and helped edit the manuscript. E.N.C. designed and carried out native PAGE experiment, analyzed data, and helped edit the manuscript. G.S.S. helped with AFM experimental design and data interpretation, and with editing the manuscript. K.C.W. designed and carried out experiments,

analyzed data, and helped edit the manuscript. V.P.D. contributed to designing experimental plans and helped edit the manuscript. W.L.K. contributed to experimental plans, consulted on data interpretation, provided guidance, and revised the manuscript.

## ■ Funding

This work was supported by grants from the National Science Foundation Award Numbers EEC-0647560, CMMI-0926019, and ECCS-0925882 (V.P.D.) and National Institutes of Health-National Institute of Aging Grants AG022547 and AG029460 (W.L.K.). A.S. was a recipient of a postdoctoral fellowship from CNPq-Brazil.

## ■ Notes

The authors declare the following competing financial interest(s): WLK is co-founder of Acumen Pharmaceuticals, which has been licensed by Northwestern University to target ADDLs (A-Derived Diffusible Ligands with dementing action) for Alzheimers therapeutics and diagnostics.

## ■ ACKNOWLEDGMENTS

We thank Jane Wang and Summer Wu for their assistance in the immunolabeling of hippocampal cells and conjugation of NU4 antibody, respectively. AFM imaging was performed in the NIFTI facility in the NUANCE center at Northwestern University, which is supported by NSF-NSEC, NSF-MRSEC, Keck Foundation, the State of Illinois and Northwestern University.

## ■ ABBREVIATIONS

$A\beta$ , amyloid  $\beta$ ; AD, Alzheimer's disease;  $A\beta\text{O}$ ,  $A\beta$  oligomer; HPLC, high performance liquid chromatography; SEC, size-exclusion chromatography; AFM, atomic force microscopy; PBS, phosphate buffered saline; TBS, Tris-buffer saline; TBS-T, TBS with Tween-20

## ■ REFERENCES

- (1) Thies, W., Bleiler, L., and Assoc, A. s. (2013) 2013 Alzheimer's disease facts and figures Alzheimer's Association. *Alzheimer's Dementia* 9, 208–245.
- (2) Gralle, M., and Ferreira, S. T. (2007) Structure and functions of the human amyloid precursor protein: The whole is more than the sum of its parts. *Prog. Neurobiol.* 82, 11–32.
- (3) Klein, W. L., Krafft, G. A., and Finch, C. E. (2001) Targeting small A beta oligomers: The solution to an Alzheimer's disease conundrum? *Trends Neurosci.* 24, 219–224.
- (4) Hardy, J., and Selkoe, D. J. (2002) Medicine - The amyloid hypothesis of Alzheimer's disease: Progress and problems on the road to therapeutics. *Science* 297, 353–356.
- (5) Lambert, M. P., Barlow, A. K., Chromy, B. A., Edwards, C., Freed, R., Liosatos, M., Morgan, T. E., Rozovsky, I., Trommer, B., Viola, K. L., Wals, P., Zhang, C., Finch, C. E., Krafft, G. A., and Klein, W. L. (1998) Diffusible, nonfibrillar ligands derived from A beta(1–42) are potent central nervous system neurotoxins. *Proc. Natl. Acad. Sci. U.S.A.* 95, 6448–6453.
- (6) Krafft, G. A., and Klein, W. L. (2010) ADDLs and the signaling web that leads to Alzheimer's disease. *Neuropharmacology* 59, 230–242.
- (7) Benilova, I., Karran, E., and De Strooper, B. (2012) The toxic A beta oligomer and Alzheimer's disease: An emperor in need of clothes. *Nat. Neurosci.* 15, 349–357.
- (8) Broersen, K., Rousseau, F., and Schymkowitz, J. (2010) The culprit behind amyloid beta peptide related neurotoxicity in Alzheimer's disease: Oligomer size or conformation? *Alzheimer's Res. Ther.* 2, 12.

- (9) Benilova, I., and De Strooper, B. (2011) An overlooked neurotoxic species in Alzheimer's disease. *Nat. Neurosci.* 14, 949–950.
- (10) Reed, M. N., Hofmeister, J. J., Jungbauer, L., Welzel, A. T., Yu, C. J., Sherman, M. A., Lesne, S., LaDu, M. J., Walsh, D. M., Ashe, K. H., and Cleary, J. P. (2011) Cognitive effects of cell-derived and synthetically derived A beta oligomers. *Neurobiol. Aging* 32, 1784–1794.
- (11) Figueiredo, C. P., Clarke, J. R., Ledo, J. H., Ribeiro, F. C., Costa, C. V., Melo, H. M., Mota-Sales, A. P., Saraiva, L. M., Klein, W. L., Sebollela, A., De Felice, F. G., and Ferreira, S. T. (2013) Memantine rescues transient cognitive impairment caused by high-molecular-weight abeta oligomers but not the persistent impairment induced by low-molecular-weight oligomers. *J. Neurosci.* 33, 9626–9634.
- (12) Walsh, D. M., Klyubin, I., Fadeeva, J. V., Cullen, W. K., Anwyl, R., Wolfe, M. S., Rowan, M. J., and Selkoe, D. J. (2002) Naturally secreted oligomers of amyloid beta protein potently inhibit hippocampal long-term potentiation in vivo. *Nature* 416, 535–539.
- (13) Cleary, J. P., Walsh, D. M., Hofmeister, J. J., Shankar, G. M., Kuskowski, M. A., Selkoe, D. J., and Ashe, K. H. (2005) Natural oligomers of the amyloid-protein specifically disrupt cognitive function. *Nat. Neurosci.* 8, 79–84.
- (14) Shankar, G. M., Li, S. M., Mehta, T. H., Garcia-Munoz, A., Shepardson, N. E., Smith, I., Brett, F. M., Farrell, M. A., Rowan, M. J., Lemere, C. A., Regan, C. M., Walsh, D. M., Sabatini, B. L., and Selkoe, D. J. (2008) Amyloid-beta protein dimers isolated directly from Alzheimer's brains impair synaptic plasticity and memory. *Nat. Med.* 14, 837–842.
- (15) Cizas, P., Budvytyte, R., Morkuniene, R., Moldovan, R., Broccio, M., Losche, M., Niaura, G., Valincius, G., and Borutaite, V. (2010) Size-dependent neurotoxicity of beta-amyloid oligomers. *Arch. Biochem. Biophys.* 496, 84–92.
- (16) Brouillette, J., Caillierez, R., Zommer, N., Alves-Pires, C., Benilova, I., Blum, D., De Strooper, B., and Buee, L. (2012) Neurotoxicity and Memory Deficits Induced by Soluble Low-Molecular-Weight Amyloid-beta(1–42) Oligomers Are Revealed In Vivo by Using a Novel Animal Model. *J. Neurosci.* 32, 7852–7861.
- (17) Gong, Y. S., Chang, L., Viola, K. L., Lacor, P. N., Lambert, M. P., Finch, C. E., Krafft, G. A., and Klein, W. L. (2003) Alzheimer's disease-affected brain: Presence of oligomeric A beta ligands (ADDLs) suggests a molecular basis for reversible memory loss. *Proc. Natl. Acad. Sci. U.S.A.* 100, 10417–10422.
- (18) Lacor, P. N., Buniel, M. C., Chang, L., Fernandez, S. J., Gong, Y. S., Viola, K. L., Lambert, M. P., Velasco, P. T., Bigio, E. H., Finch, C. E., Krafft, G. A., and Klein, W. L. (2004) Synaptic targeting by Alzheimer's-related amyloid beta oligomers. *J. Neurosci.* 24, 10191–10200.
- (19) Lesne, S., Koh, M. T., Kotilinek, L., Kaye, R., Glabe, C. G., Yang, A., Gallagher, M., and Ashe, K. H. (2006) A specific amyloid-beta protein assembly in the brain impairs memory. *Nature* 440, 352–357.
- (20) Fukumoto, H., Tokuda, T., Kasai, T., Ishigami, N., Hidaka, H., Kondo, M., Allsop, D., and Nakagawa, M. (2010) High-molecular-weight beta-amyloid oligomers are elevated in cerebrospinal fluid of Alzheimer patients. *FASEB J.* 24, 2716–2726.
- (21) Ahmed, M., Davis, J., Aucoin, D., Sato, T., Ahuja, S., Aimoto, S., Elliott, J. I., Van Nostrand, W. E., and Smith, S. O. (2010) Structural conversion of neurotoxic amyloid-beta(1–42) oligomers to fibrils. *Nat. Struct. Mol. Biol.* 17, 561–U556.
- (22) Barghorn, S., Nimmrich, V., Striebinger, A., Krantz, C., Keller, P., Janson, B., Bahr, M., Schmidt, M., Bitner, R. S., Harlan, J., Barlow, E., Ebert, U., and Hillen, H. (2005) Globular amyloid beta-peptide(1–42) oligomer—A homogenous and stable neuropathological protein in Alzheimer's disease. *J. Neurochem.* 95, 834–847.
- (23) Durakoglugil, M. S., Chen, Y., White, C. L., Kavalali, E. T., and Herz, J. (2009) Reelin signaling antagonizes beta-amyloid at the synapse. *Proc. Natl. Acad. Sci. U.S.A.* 106, 15938–15943.
- (24) Noguchi, A., Matsumura, S., Dezawa, M., Tada, M., Yanazawa, M., Ito, A., Akioka, M., Kikuchi, S., Sato, M., Ideno, S., Noda, M., Fukunari, A., Muramatsu, S., Itokazu, Y., Sato, K., Takahashi, H., Teplow, D. B., Nabeshima, Y., Kakita, A., Imahori, K., and Hoshi, M. (2009) Isolation and Characterization of Patient-derived, Toxic, High Mass Amyloid beta-Protein (A beta) Assembly from Alzheimer Disease Brains. *J. Biol. Chem.* 284, 32895–32905.
- (25) Lee, E. B., Leng, L. Z., Zhang, B., Kwong, L., Trojanowski, J. Q., Abel, T., and Lee, V. M. Y. (2006) Targeting amyloid-beta peptide (A beta) oligomers by passive immunization with a conformation-selective monoclonal antibody improves learning and memory in A beta precursor protein (APP) transgenic mice. *J. Biol. Chem.* 281, 4292–4299.
- (26) Lambert, M. P., Velasco, P. T., Chang, L., Viola, K. L., Fernandez, S., Lacor, P. N., Khuon, D., Gong, Y. S., Bigio, E. H., Shaw, P., De Felice, F. G., Krafft, G. A., and Klein, W. L. (2007) Monoclonal antibodies that target pathological assemblies of A beta. *J. Neurochem.* 100, 23–35.
- (27) Lambert, M. P., Velasco, P. T., Viola, K. L., and Klein, W. L. (2009) Targeting Generation of Antibodies Specific to Conformational Epitopes of Amyloid beta-Derived Neurotoxins. *CNS Neurol. Disord.: Drug Targets* 8, 65–81.
- (28) Xiao, C., Davis, F. J., Chauhan, B. C., Viola, K. L., Lacor, P. N., Velasco, P. T., Klein, W. L., and Chauhan, N. B. (2013) Brain transit and ameliorative effects of intranasally delivered anti-amyloid-beta oligomer antibody in 5XFAD mice. *J. Alzheimer's Dis.* 35, 777–788.
- (29) Klein, W. L. (2002) Abeta toxicity in Alzheimer's disease: Globular oligomers (ADDLs) as new vaccine and drug targets. *Neurochem. Int.* 41, 345–352.
- (30) Bhaskar, K., Miller, M., Chludzinski, A., Herrup, K., Zagorski, M., and Lamb, B. T. (2009) The PI3K-Akt-mTOR pathway regulates Abeta oligomer induced neuronal cell cycle events. *Mol. Neurodegener.* 4, 14.
- (31) Chromy, B. A., Nowak, R. J., Lambert, M. P., Viola, K. L., Chang, L., Velasco, P. T., Jones, B. W., Fernandez, S. J., Lacor, P. N., Horowitz, P., Finch, C. E., Krafft, G. A., and Klein, W. L. (2003) Self-assembly of A beta(1–42) into globular neurotoxins. *Biochemistry* 42, 12749–12760.
- (32) Sebollela, A., Freitas-Correa, L., Oliveira, F. F., Paula-Lima, A. C., Saraiva, L. M., Martins, S. M., Mota, L. D., Torres, C., Alves-Leon, S., de Souza, J. M., Carraro, D. M., Brentani, H., De Felice, F. G., and Ferreira, S. T. (2012) Amyloid-beta Oligomers Induce Differential Gene Expression in Adult Human Brain Slices. *J. Biol. Chem.* 287, 7436–7445.
- (33) Velasco, P. T., Heffern, M. C., Sebollela, A., Popova, I. A., Lacor, P. N., Lee, K. B., Sun, X., Tiano, B. N., Viola, K. L., Eckermann, A. L., Meade, T. J., and Klein, W. L. (2012) Synapse-binding subpopulations of Abeta oligomers sensitive to peptide assembly blockers and scFv antibodies. *ACS Chem. Neurosci.* 3, 972–981.
- (34) Lambert, M. P., Viola, K. L., Chromy, B. A., Chang, L., Morgan, T. E., Yu, J. X., Venton, D. L., Krafft, G. A., Finch, C. E., and Klein, W. L. (2001) Vaccination with soluble A beta oligomers generates toxicity-neutralizing antibodies. *J. Neurochem.* 79, 595–605.
- (35) Prin, C., Bene, M. C., Gobert, B., Montagne, P., and Faure, G. C. (1995) Isoelectric restriction of human immunoglobulin isotypes. *Biochim. Biophys. Acta* 1243, 287–289.
- (36) San Paulo, A., and Garcia, R. (2000) High-resolution imaging of antibodies by tapping-mode atomic force microscopy: Attractive and repulsive tip-sample interaction regimes. *Biophys. J.* 78, 1599–1605.
- (37) Martinez, N. F., Lozano, J. R., Herruzo, E. T., Garcia, F., Richter, C., Sulzbach, T., and Garcia, R. (2008) Bimodal atomic force microscopy imaging of isolated antibodies in air and liquids. *Nanotechnology* 19, 384011.
- (38) Porath, J. (1963) Some recently developed fractionation procedures and their application to peptide and protein hormones. *Pure Appl. Chem.* 6, 233–244.
- (39) Bhushan, B., Tokachichu, D. R., Keener, M. T., and Lee, S. C. (2005) Morphology and adhesion of biomolecules on silicon based surfaces. *Acta Biomater* 1, 327–341.
- (40) Bolshakova, A. V., Kiselyova, O. I., Filonov, A. S., Frolova, O. Y., Lyubchenko, Y. L., and Yaminsky, I. V. (2001) Comparative studies of

bacteria with an atomic force microscopy operating in different modes. *Ultramicroscopy* 86, 121–128.

(41) Shekhawat, G. S., Lambert, M. P., Sharma, S., Velasco, P. T., Viola, K. L., Klein, W. L., and Dravid, V. P. (2009) Soluble state high resolution atomic force microscopy study of Alzheimer's beta-amyloid oligomers. *Appl. Phys. Lett.*, 95.

(42) Mustata, G. M., Shekhawat, G. S., Lambert, M. P., Viola, K. L., Velasco, P. T., Klein, W. L., and Dravid, V. P. (2012) Insights into the mechanism of Alzheimer's beta-amyloid aggregation as a function of concentration by using atomic force microscopy. *Appl. Phys. Lett.* 100, 133704.

(43) Pitt, J., Roth, W., Lacor, P., Smith, A. B., Blankenship, M., Velasco, P., De Felice, F., Breslin, P., and Klein, W. L. (2009) Alzheimer's-associated A beta oligomers show altered structure, immunoreactivity and synaptotoxicity with low doses of oleocanthal. *Toxicol. Appl. Pharmacol.* 240, 189–197.

(44) Brewer, G. J., Torricelli, J. R., Evege, E. K., and Price, P. J. (1993) Optimized Survival of Hippocampal-Neurons in B27-Supplemented Neurobasal, a New Serum-Free Medium Combination. *J. Neurosci. Res.* 35, 567–576.